KRIGING-BASED FINITE ELEMENT METHODS FOR ANALYSES OF SHEAR DEFORMABLE BEAMS AND PLATES

F.T. Wong

Petra Christian University, Surabaya, Indonesia, wftjong@petra.ac.id

ABSTRACT

An enhancement of the finite element method using Kriging interpolation (K-FEM) has been recently developed. The key advantage of this innovative method is that the polynomial refinement can be performed without adding nodes or changing the element connectivity. This paper presents the development of the K-FEM for analyses of shear deformable beams and plates. The discretized equations are formulated using the standard displacement-based finite element procedure on the variational equations of Timoshenko beam and Reissner-Mindlin plate. The transverse displacement and the rotations of the beam and the plates are independently approximated using Kriging interpolation. For each element, the interpolation function is constructed from a set of nodes within a prescribed domain of influence comprising the element and its several layers of neighbouring elements. The cubic or quartic polynomial basis functions are utilized to alleviate the shear locking. A series of numerical tests are performed to examine the developed Kriging-based beam and plate elements. The results demonstrate that for the case in which shear locking is not an issue, the elements perform very well.

Key words: Finite element, Kriging, Timoshenko beam, Reissner-Mindlin plate

INTRODUCTION

A new variant of the finite element method what so-called Kriging-based finite element method (K-FEM) was introduced by Plengkhom & Kanok-Nukulchai (2005). In this method, Kriging interpolation (KI) is employed as the trial function in place of the conventional polynomial function. The KI is constructed for each element using a set of nodes in a domain of influencing nodes (DOI) composed of several layers of elements (the DOI is in the form of polygon for 2D problems). Combining the KI of all elements, the global field variable is thus approximated by piecewise KI (Wong & Kanok-Nukulchai, 2009a; Wong & Syamsoeyadi, 2011)

The advantages of the K-FEM are: (1). highly-accurate and smooth field variables and their gradients can be obtained even using the simplest form of elements (triangles in the 2D domain and tetrahedrons in the 3D domain). (2). The polynomial refinement can be achieved without any change to the element or mesh structure. (3). The formulation and coding of the K-FEM are very similar to the conventional FEM so that any existing general-purpose FE program can be easily extended to incorporate the enhanced method. Thus, the K-FEM has a high chance to be accepted in real engineering practices.

In the pioneering work of Plengkhom & Kanok-Nukulchai (2005), the K-FEM was developed for static analyses of 1D bar and 2D plane-stress/plane-strain solids. Subsequently, it was developed for analyses of Reissner-Mindlin plates (Wong & Kanok-Nukulchai, 2006) and improved through the use of adaptive correlation parameters and by introducing the quartic spline correlation function. A drawback of the K-FEM is that the interpolation function is discontinuous at the inter-element boundaries (except in 1D problems). In spite of this discontinuity, using appropriate choice of shape function parameters, the K-FEM passes weak patch tests and therefore the convergence is guaranteed (Wong & Kanok-Nukulchai, 2009b). The basic concepts and advances of the K-FEM have been presented in several papers (Kanok-Nukulchai & Wong, 2008; Wong & Kanok-Nukulchai, 2009a; Wong, 2011). The current development is the extension and application of the K-FEM to different problems in engineering, such as general plate and shell structures (Wong, 2009) and multi-scale mechanics (Sommanawat & Kanok-Nukulchai, 2009).

This paper reviews the K-FEM for analyses of shear deformable beams and plates, i.e. Timoshenko beam and (K-Beam) and Reissnes-Mindlin plate (K-Plate) elements. The KI, formulation of the elements, and numerical testing results are presented.

KRIGING INTERPOLATION IN THE K-FEM

Consider a continuous field variable $u(\mathbf{x})$ defined in a domain Ω. The domain is represented by a set of properly scattered nodes $\mathbf{x}_i$, i=1, 2, …, N, where N is the total number of nodes in the whole domain. Given N field values $u(\mathbf{x}_1)$, …, $u(\mathbf{x}_N)$, the problem of interest is to obtain an estimated value of u at a point $\mathbf{x}_0 \in \Omega$.

The Kriging estimated value $u^{\mathrm{h}}(\mathbf{x}_0)$ is a linear combination of $u(\mathbf{x}_1)$, …, $u(\mathbf{x}_n)$, i.e.

$$u^{\mathrm{h}}(\mathbf{x}_0) = \sum_{i=1}^{n} \lambda_i u(\mathbf{x}_i) \tag{1}$$

where λ_i's are the unknown *Kriging weights* and n is the number of nodes surrounding point $\mathbf{x}_0$, inside and on the boundary of a DOI $\Omega_{\mathbf{x}0} \subseteq \Omega$. Considering each function values $u(\mathbf{x}_1)$, …, $u(\mathbf{x}_n)$ as the realizations of random variables $U(\mathbf{x}_1)$, …, $U(\mathbf{x}_n)$, Eq. (1) can be written as

$$U^{\mathrm{h}}(\mathbf{x}_0) = \sum_{i=1}^{n} \lambda_i U(\mathbf{x}_i) \tag{2}$$

The Kriging weights are determined by requiring the estimator $U^{\mathrm{h}}(\mathbf{x}_0)$ unbiased, i.e.

$$\mathrm{E}\left[U^{\mathrm{h}}(\mathbf{x}_0) - U(\mathbf{x}_0)\right] = 0 \tag{3}$$

where $\mathrm{E}[\bullet]$ is the expected value operator, and by minimizing the variance of estimation error, $\mathrm{var}\left[U^{\mathrm{h}}(\mathbf{x}_0) - U(\mathbf{x}_0)\right]$. Using the method of Lagrange for the constraint optimization problem, the requirements of minimum variance and unbiased estimator lead to the following Kriging equation system (see Wong (2009) for the complete derivation):

$$\begin{aligned} \mathbf{R}\boldsymbol{\lambda} + \mathbf{P}\boldsymbol{\mu} &= \mathbf{r}(\mathbf{x}_0) \\ \mathbf{P}^{\mathrm{T}}\boldsymbol{\lambda} &= \mathbf{p}(\mathbf{x}_0) \end{aligned} \tag{4}$$

in which

$$\mathbf{R} = \begin{bmatrix} C(\mathbf{h}_{11}) & \dots & C(\mathbf{h}_{1n}) \\ \dots & \dots & \dots \\ C(\mathbf{h}_{n1}) & \dots & C(\mathbf{h}_{nn}) \end{bmatrix}; \qquad \mathbf{P} = \begin{bmatrix} p_1(\mathbf{x}_1) & \dots & p_m(\mathbf{x}_1) \\ \dots & \dots & \dots \\ p_1(\mathbf{x}_n) & \dots & p_m(\mathbf{x}_n) \end{bmatrix};$$

$$\boldsymbol{\lambda} = \begin{bmatrix} \lambda_1 & \dots & \lambda_n \end{bmatrix}^{\mathrm{T}}; \qquad \boldsymbol{\mu} = \begin{bmatrix} \mu_1 & \dots & \mu_m \end{bmatrix}^{\mathrm{T}}$$

$$\mathbf{r}(\mathbf{x}_0) = \begin{bmatrix} C(\mathbf{h}_{10}) & C(\mathbf{h}_{20}) & \dots & C(\mathbf{h}_{n0}) \end{bmatrix}^{\mathrm{T}}; \qquad \mathbf{p}(\mathbf{x}_0) = \begin{bmatrix} p_1(\mathbf{x}_0) & \dots & p_m(\mathbf{x}_0) \end{bmatrix}^{\mathrm{T}}$$

R is an $n \times n$ matrix of covariance of $U(\mathbf{x})$ at nodes $\mathbf{x}_1$, …, $\mathbf{x}_n$; **P** is an $n \times m$ matrix of polynomial values at the nodes; $\boldsymbol{\lambda}$ is an $n \times 1$ vector of Kriging weights; $\boldsymbol{\mu}$ is an $m \times 1$ vector of Lagrange multipliers; $\mathbf{r}(\mathbf{x}_0)$ is an $n \times 1$ vector of covariance between the nodes and the node of interest, $\mathbf{x}_0$; and $\mathbf{p}(\mathbf{x}_0)$ is an $m \times 1$ vector of polynomial basis at $\mathbf{x}_0$. While $C(\mathbf{h}_{ij}) = \mathrm{cov}\left[U(\mathbf{x}_i), U(\mathbf{x}_j)\right]$ is the covariance between $U(\mathbf{x})$ at node $\mathbf{x}_i$ and $U(\mathbf{x})$ at node $\mathbf{x}_j$. The unknown Kriging weights $\boldsymbol{\lambda}$ and Lagrange multipliers $\boldsymbol{\mu}$ are obtained by solving the Kriging equations, Eqs. (4).

Since the point of interest $\mathbf{x}_0$ can be any point in the DOI, the symbol $\mathbf{x}_0$ in Eq. (1) can be replaced by symbol $\mathbf{x}$. Thus, using the usual finite element symbol, Eq. (1) can be expressed as

$$u^{\mathrm{h}}(\mathbf{x}) = \sum_{i=1}^{n} N_i(\mathbf{x})\, u_i = \mathbf{N}(\mathbf{x})\mathbf{d} \tag{5}$$

where $\mathbf{N}(\mathbf{x})=[\ N_1(\mathbf{x})\ \ ...\ \ N_n(\mathbf{x})\ ]=[\ \lambda_1(\mathbf{x})\ \ ...\ \ \lambda_n(\mathbf{x})\ ]$ is the $1 \times n$ shape function matrix and $\mathbf{d}=[u(\mathbf{x}_1)\ \ ...\ \ u(\mathbf{x}_n)]^{\mathrm{T}}$ is an $n \times 1$ vector of nodal values.

In order to construct Kriging shape functions in Eq. (5), a polynomial basis function and a correlation function should be chosen. Basis functions ranging from polynomial of the degree one up to four have been utilized in the past works on the K-FEM. In the problems of shear deformable beam, plate and shell, it is necessary to use cubic or quartic polynomial basis in order to alleviate the shear or membrane locking (Wong & Syamsoeyadi, 2011; Wong, 2009).

Covariance between a pair of random variables $U(\mathbf{x})$ and $U(\mathbf{x}+\mathbf{h})$ can be expressed in terms of correlation coefficient function or shortly, correlation function, i.e. $\rho(\mathbf{h}) = C(\mathbf{h})/\sigma^2$, where $\sigma^2 = \mathrm{var}[U(\mathbf{x})]$ and $\mathbf{h}$ is a vector separating two points $\mathbf{x}$ and $\mathbf{x}+\mathbf{h}$. In the K-FEM, factor σ^2 has no effect on the final results and it was taken equal to 1 in this study. The correlation functions that have been utilized in the previous works are Gaussian, viz.

$$\rho(\mathbf{h}) = \rho(h) = \exp(-(\theta h/d)^2) \tag{6}$$

and Quartic Spline, viz.

$$\rho(\mathbf{h}) = \rho(h) = \begin{cases} 1-6(\theta h/d)^2 + 8(\theta h/d)^3 - 3(\theta h/d)^4 & \text{for } 0 \le \theta h/d \le 1 \\ 0 & \text{for } \theta h/d > 1 \end{cases} \tag{7}$$

In these equations, $\theta>0$ is the correlation parameter, $h = \|\mathbf{h}\|$, i.e. the Euclidean distance between points $\mathbf{x}$ and $\mathbf{x}+\mathbf{h}$, and d is a scale factor to normalize the distance. In this study, the correlation parameter was chosen based on the results of the search for the lower and upper bound values of θ (Wong & Kanok-Nukulchai, 2009b; Wong & Syamsoeyadi, 2011) satisfying the rule of thumb given by Plengkhom & Kanok-Nukulchai (2005). Factor d was taken to be the largest distance between any pair of nodes in the DOI.

FORMULATION OF KRIGING-BASED TIMOSHENKO BEAM ELEMENT

The variational governing equation for static deflection of Timoshenko beam (Friedman & Kosmatka, 1993) is

$$\int_0^L \delta\psi_{,x}\, EI\psi_{,x}\, dx + \int_0^L (\delta w_{,x} - \delta\psi)\, kGA(w_{,x} - \psi) dx = \int_0^L \delta w\, q dx + \int_0^L \delta\psi\, m dx \tag{8}$$

The primary variables in this equation are the transverse displacement (deflection) of the neutral axis of the beam, w, and the rotation of the cross-section, ψ, which are functions of independent variables coordinate x. The external forces acting on the beam are the distributed force along the length of the beam, q, and distributed moment, m. The geometrical parameters are the length of the beam, L, the cross-sectional area, A, and the moment of inertia, I. The material properties are Young's modulus, E, and the shear modulus, G. The other parameter is k, i.e a shear correction factor, which is dependent upon the cross-section geometry. The symbol δ is the variational operator, so that δw and $\delta\psi$ are the admissible variations of w and ψ, respectively (also called virtual displacements). The comma denotes the first partial derivative with respect to the variable that follows (i.e. x).

Suppose a beam is divided into a number of finite elements. For each element, KI is constructed based upon a set of nodes in a DOI including the element itself and a predetermined number of neighbouring elements (see Wong & Kanok-Nukulchai (2009a) and Wong (2011) for detailed explanations). Consider now an element with its DOI including n nodes. The displacement components over the element are approximated by KI as follows:

$$w = \mathbf{N}_{\mathbf{w}}\,\mathbf{d}\ ;\quad \psi = \mathbf{N}_{\psi}\,\mathbf{d} \tag{9}$$

where $\mathbf{N}_{\mathbf{w}} = \{N_1\ \ 0\ \ N_2\ \ 0\ \ \cdots\ \ N_n\ \ 0\}$, $\mathbf{N}_{\psi} = \{0\ \ N_1\ \ 0\ \ N_2\ \ \cdots\ \ 0\ \ N_n\}$, and $\mathbf{d} = \{w_1\ \ \psi_1\ \ w_2\ \ \psi_2\ \ \cdots\ \ w_n\ \ \psi_n\}^T$. Here the shape functions (N_1, N_2, ..., N_n) are Kriging shape functions, which are obtained by solving Kriging equations, Eqs. (4).

Substituting the approximated displacement functions Eqs. (9) into the variational equation, Eq. (8), leads to the discrete equation $\mathbf{kd} = \mathbf{f}$, in which

$$\mathbf{k} = \int_0^L \mathbf{N}_{\psi,x}^{\mathrm{T}}\, EI\, \mathbf{N}_{\psi,x}\, dx \;+\; \int_0^L \left(\mathbf{N}_{w,x} - \mathbf{N}_{\psi}\right)^{\mathrm{T}} kGA\left(\mathbf{N}_{w,x} - \mathbf{N}_{\psi}\right) dx \tag{10}$$

is the element stiffness matrix, and

$$\mathbf{f} = \int_0^L \mathbf{N}_{\mathrm{w}} q\, dx + \int_0^L \mathbf{N}_{\psi}\, m\, dx \tag{11}$$

is the element equivalent nodal force vector. The size of the matrices **k**, **d**, and **f** depends on the number of nodes in the DOI, n. The integrations in Eqs. (10) and (11) are evaluated using Gauss quadrature. The selective-reduced integration technique (SRI) (Hughes, Taylor, & Kanoknukulchai, 1977) can be employed to overcome the shear locking phenomenon.

FORMULATION OF KRIGING-BASED REISSNER-MINDLIN PLATE ELEMENT

Consider a plate of uniform thickness, h, homogeneous, referred to a three-dimensional Cartesian co-ordinate system with the x-y plane lying on the middle surface of the plate (Fig. 1). The primary variables in the RM plate problem are the deflection of a point initially lying on the neutral plane, w, and the components of rotation of a normal line, namely ψ_x and ψ_y. The positive sign convention for these rotation components and displacement components is showed in Fig. 1.

The variational governing equation for static deflection of RM plate under transversal load $q(x, y)$ (Wong, 2009) is

$$\int_S \delta\boldsymbol{\kappa}^{\mathrm{T}} \mathbf{D}_{\mathrm{b}} \boldsymbol{\kappa}\, dS + \int_S \delta\boldsymbol{\varepsilon}_{\mathrm{s}}^{\mathrm{T}} \mathbf{D}_{\mathrm{s}} \boldsymbol{\varepsilon}_{\mathrm{s}}\, dS = \int_S \delta\mathbf{u}^{\mathrm{T}} \mathbf{p}\, dS \tag{12}$$

In this equation,

$$\boldsymbol{\kappa} = \begin{Bmatrix} \psi_{x,x} \\ \psi_{y,y} \\ \psi_{x,y} + \psi_{y,x} \end{Bmatrix}; \quad \boldsymbol{\epsilon}_{\mathrm{s}} = \begin{Bmatrix} \gamma_{xz} \\ \gamma_{yz} \end{Bmatrix} \tag{13}$$

are the vector of curvatures and the vector of tranverse shear strains, respectively,

$$\mathbf{u}^{\mathrm{T}} = \{w \quad \psi_x \quad \psi_y\} \tag{14}$$

is the vector of the primary variables, i.e. the deflection and rotation components, and

$$\mathbf{p} = \{q \quad 0 \quad 0\}^{\mathrm{T}} \tag{15}$$

is the vector of external loads.

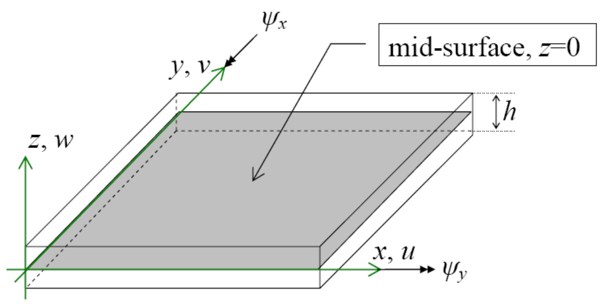

Fig. 1: Plate, coordinate system, and positive directions for displacement and rotation components

For a linear-elastic and isotropic material with the elastic modulus E and Poisson's ratio ν:

$$\mathbf{D}_\mathrm{b} = \frac{Eh^3}{12(1-\nu^2)}\begin{bmatrix} 1 & \nu & 0 \\ \nu & 1 & 0 \\ 0 & 0 & \frac{1}{2}(1-\nu) \end{bmatrix} = D_\mathrm{b}\begin{bmatrix} 1 & \nu & 0 \\ \nu & 1 & 0 \\ 0 & 0 & \frac{1}{2}(1-\nu) \end{bmatrix} \tag{16}$$

$$\mathbf{D}_\mathrm{s} = Gkh\begin{bmatrix} 1 & 0 \\ 0 & 1 \end{bmatrix} = D_\mathrm{s}\begin{bmatrix} 1 & 0 \\ 0 & 1 \end{bmatrix} \tag{17}$$

Factors D_b in Eq. (16) and D_s in Eq (17) are the bending (or flexural) rigidity and the shear rigidity of the plate, respectively. Factor G is the shear modulus and k is shear correction factor, which is equal to 5/6 for a homogeneous plate.

Suppose the domain S is subdivided into a mesh of N_el triangular elements and N nodes. To obtain an approximate solution using the concept of KI with layered-element DOI, for each element e=1, 2, …, N_el the plate field variables are approximated by the KI as follows:

$$w = \textstyle\sum_i^n N_i(x,y)w_i \; ; \quad \psi_x = \sum_i^n N_i(x,y)\psi_{xi} \; ; \quad \psi_y = \sum_i^n N_i(x,y)\psi_{yi} \tag{18}$$

Here $N_i(x,y)$ is Kriging shape functions associated with node i for approximating defection, rotation in the -y-direction, and rotation in the x-direction, respectively; w_i, ψ_{xi} and ψ_{yi} are nodal deflection, nodal rotation in the –y-direction, and nodal rotation in the x-direction, respectively; n is the number of nodes in the DOI of an element, which generally varies from element to element.

Substituting the approximated displacement functions Eqs. (18) into the variational equation, Eq. (12), leads to the discrete equation **kd**=**f,** in which

$$\mathbf{k} = \mathbf{k}_\mathrm{b} + \mathbf{k}_\mathrm{s} = \int_S \mathbf{B}_\mathrm{b}^\mathrm{T}\mathbf{D}_\mathrm{b}\mathbf{B}_\mathrm{b}\,dS + \int_S \mathbf{B}_\mathrm{s}^\mathrm{T}\mathbf{D}_\mathrm{s}\mathbf{B}_\mathrm{s}\,dS \tag{19}$$

is the element stiffness matrix, $\mathbf{d} = \{w_1 \quad \psi_{x1} \quad \psi_{y1} \quad w_2 \quad \psi_{x2} \quad \psi_{y2} \quad \cdots \quad w_n \quad \psi_{xn} \quad \psi_{yn}\}^\mathrm{T}$ is the element nodal displacement vector, and

$$\mathbf{f} = \int_S \mathbf{N}^\mathrm{T}\mathbf{p}\,dS \tag{20}$$

is the element nodal force vector. In Eq. (19), $\mathbf{k}_\mathrm{b}$ and $\mathbf{k}_\mathrm{s}$ are the bending and the transverse shear stiffness matrices, respectively,

$$\mathbf{B}_\mathrm{b} = \begin{bmatrix} 0 & N_{1,x} & 0 & \cdots & 0 & N_{n,x} & 0 \\ 0 & 0 & N_{1,y} & \cdots & 0 & 0 & N_{n,y} \\ 0 & N_{1,y} & N_{1,x} & \cdots & 0 & N_{n1,y} & N_{n,x} \end{bmatrix} \tag{21}$$

is the curvature-displacement matrix, and

$$\mathbf{B}_\mathrm{s} = \begin{bmatrix} N_{1,x} & -N_1 & 0 & \cdots & N_{n,x} & -N_n & 0 \\ N_{1,y} & 0 & -N_1 & \cdots & N_{n,y} & 0 & -N_n \end{bmatrix} \tag{22}$$

is the shear strain-displacement matrix. In Eq. (20),

$$\mathbf{N} = \begin{bmatrix} N_1 & 0 & 0 & \cdots & N_n & 0 & 0 \\ 0 & N_1 & 0 & \cdots & 0 & N_n & 0 \\ 0 & 0 & N_1 & \cdots & 0 & 0 & N_n \end{bmatrix} \tag{23}$$

is the shape function matrix.

NUMERICAL RESULTS

Beam Element

To test the performance of the developed K-Beam, a cantilever beam subjected to triangular-distributed load as shown in Fig. 2 was analyzed using the K-Beam with cubic polinomial basis, three-layer DOI, and Gaussian correlation function (P3-3-G). The geometrical and material parameters of the beam are E=1000 kN/m^2, I=0.020833 m^4, A=1 m^2, G=384.61 kN/m^2, k=0.84967, ν=0.3, L=4 m, L/h=8. The beam was divided into 4, 8, and 16 elements. The shape function parameter θ was taken to be equal to 1. The number of the integration sampling points for evaluating the stiffness matrices (Eq. 10) was taken to be equal to 3 while for evaluating the force vector (Eq. 11) was taken to be equal to 2. In the case where the SRI technique was employed, the number of sampling points for the bending term was 3 while that for the shearing term was 1.

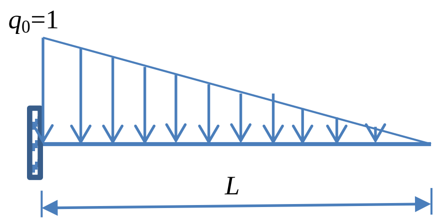

Fig. 2: Cantilever beam subjected to unit triangular distributed load

The deflections at the free end, the bending moments and the shearing forces at the clamped end were observed. The results were normalized with respect to their respective exact solutions and presented in Tables 1-3 together with the results of the superconvergent beam element of Friedman & Kosmatka (1993) (F&K). The tables show that both P3-3-G and P3-3-G (SRI) can produce very accurate displacements and reasonably accurate moments. The element with P3-3-G gives slightly better results than the element with SRI. The shearing forces directly calculated from the shearing strains, however, cannot produce accurate results. The use of SRI worsen the shearing forces. It is interesting to notice that the results using full integration for the displacement and moment, converge from below, while those using SRI converge from above. This is because the use of SRI makes the stiffness matrix becomes 'less stiff' than the actual.

Tab. 1: Normalized deflections at the free end

Number of elements	P3-3-G	P3-3-G (SRI)	F&K
4	0.9998	1.0042	1
8	0.9999	1.0005	1
16	0.9999	1.0000	1

Tab. 2: Normalized bending moments at the clamped end

Number of elements	P3-3-G	P3-3-G (SRI)	F&K
4	0.9350	1.0778	0.96
8	0.9924	1.0441	1
16	0.9993	1.0217	1

Tab. 3: Normalized shear forces at the clamped end

Number of elements	P3-3-G	P3-3-G (SRI)	F&K
4	1.6338	4.1432	0.8
8	1.1146	1.8706	0.9
16	1.0175	1.4110	1

Plate Element

A SS-U rhombic plate with the side length L=100, length-to-thickness ratio L/h=100, and the sharp vertex angle $\alpha=30^o$ was analysed using the K-Plate with cubic basis, three-layer DOI, quartic spline correlation function (P3-3-QS) and with quartic basis, four-layer DOI, quartic spline correlation function (P4-4-QS). The correlation parameter was adjusted to the number of nodes in the DOI of each element as presented in the paper of Wong & Kanok-Nukulchai (2006a). The mesh comprises 4×4 up to 32×32 triangular elements. Typical mesh of the plate is shown in the Fig. 3. For comparison of the K-Plate with the classical FEM, the plate was also analysed using three-node triangular element (TRI3) of Mitaim (1994). This element is a simple and efficient triangular element, developed using assumed shear strain method.

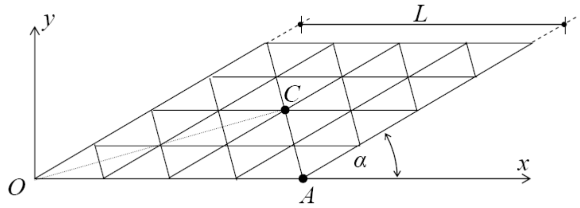

Fig. 3: Rhombic plate with mesh 4-by-4

The deflections at the center C are presented in Table 4. It shows that the results of the K-Plate are not accurate for the coarse meshes (M=4 and 8) due to shear locking. The locking, however, relieves as the mesh is finer. The results converge to the 3D solution rather than to the thin plate theory solution. This is expected since according to (Babuška & Scapolla, 1989), "the Kirchhoff model has a large error (measured in the energy norm) in comparison with the three dimensional solution with a soft simple support; also for very thin plates" and "the error of displacements of the Kirchhoff model is not negligible for $\alpha=30^o$". As a comparison, the results of TRI3 also have similar characteristic with those of the K-Plate. In this problem, the performance of the K-Plate is not better than TRI3.

Tab. 4: Center deflection of the SS-U rhombic plate with L/h=100 (x 10^{-3} qL^4/D)

M	Element Size	P3-3-QS	P4-4-QS	TRI3
4	25	0.156	0.238	0.366
8	12.5	0.355	0.355	0.388
16	6.25	0.406	0.406	0.410
32	3.125	0.419	0.419	0.419
3D solution*		0.423	0.423	0.423
Thin plate theory		0.408	0.408	0.408

M: number of divisions on each side

* Three-dimensional solution by Babuška & Scapolla (1989)

CONCLUSIONS

The K-FEM for analyses of the Timoshenko beam and Reissner-Mindlin plate has been presented. The formulation and implementation of the method are similar with the conventional FEM. The well-known shear locking problem in the FEM remains present in the present method. While the selective-reduced integration technique is applicable to K-Beam for eliminating the locking, it is not applicable to K-Plate. The numerical tests show that for thick and not very thin beams and plates, the elements can produce accurate results very accurate results in a relatively-coarse mesh. For thin plates, however, the performance of the elements is not satisfactory because of shear-locking problem. Future research on the K-Plate should be directed on developing a method to eliminate shear locking completely.

REFERENCES

Babuška, I., & Scapolla, T. (1989). Benchmark Computation and Performance Evaluation for a Rhombic Plate Bending Problem. *International Journal for Numerical Methods in Engineering*, *28*(1), 155–179. doi:10.1002/nme.1620280112

Friedman, Z., & Kosmatka, J. B. (1993). An Improved Two-node Timoshenko Beam Finite Element. *Computers & Structures*, *47*(3), 473–481. doi:10.1016/0045-7949(93)90243-7

Hughes, T. J. R., Taylor, R. L., & Kanoknukulchai, W. (1977). A Simple and Efficient Finite Element for Plate Bending. *International Journal for Numerical Methods in Engineering*, *11*(10), 1529–1543. doi:10.1002/nme.1620111005

Kanok-Nukulchai, W., & Wong, F. T. (2008). A Break-Through Enhancement of FEM Using Node-Based Kriging Interpolation. *IACM Expressions*, 24–29.

Mitaim, S. (1994). *A Family of Triangular Plate Elements Based on the Assumed Strain Method*. Asian Institute of Technology.

Plengkhom, K., & Kanok-Nukulchai, W. (2005). An Enhancement of Finite Element Method with Moving Kriging Shape Functions. *International Journal of Computational Methods*, *02*(04), 451–475. doi:10.1142/S0219876205000594

Sommanawat, W., & Kanok-Nukulchai, W. (2009). Multiscale simulation based on kriging based finite element method. *Interaction and Multiscale Mechanics*, *2*(4), 387–408. Retrieved from http://technopress.kaist.ac.kr/?page=container&journal=imm&volume=2&num=4#

Wong, F. T. (2009). *Kriging-based Finite Element Method for Analyses of Plates and Shells*. Asian Institute of Technology, Pathumthani.

Wong, F. T. (2011). A Breakthrough Enhancement of Finite Element Method using Kriging Interpolation. *Proceedings of the First Indonesian Structural Engineering and Materials Symposium* (pp. 11–1–11–16). Bandung: Parahyangan Catholic University.

Wong, F. T., & Kanok-Nukulchai, W. (2006). Kriging-based Finite Element Method for Analyses of Reissner-Mindlin plates. *Proceedings of the Tenth East-Asia Pacific Conference on Structural Engineering and Construction, Emerging Trends: Keynote Lectures and Symposia,* (pp. 509–514). Bangkok: Asian Institute of Technology.

Wong, F. T., & Kanok-Nukulchai, W. (2009a). Kriging-Based Finite Element Method : Element-By-Element Kriging Interpolation. *Civil Engineering Dimension*, *11*(1), 15–22. Retrieved from http://puslit2.petra.ac.id/ejournal/index.php/civ/article/view/17026

Wong, F. T., & Kanok-Nukulchai, W. (2009b). On the Convergence of the Kriging-based Finite Element Method. *International Journal of Computational Methods*, *06*(01), 93–118. doi:10.1142/S0219876209001784

Wong, F. T., & Syamsoeyadi, H. (2011). Kriging-based Timoshenko Beam Element for Static and Free Vibration Analyses. *Civil Engineering Dimension*, *13*(1), 42–49. Retrieved from http://puslit2.petra.ac.id/ejournal/index.php/civ/article/view/18107